

Can linear stability analyses predict the development of river bed waves with lengths much larger than the water depth?

H.J. Barneveld^{1,4}, E. Mosselman^{2,3}, V. Chavarrías², A.J.F. Hoitink¹

¹Wageningen University and Research, Hydrology and Quantitative Water Management Group, Department of Environmental Sciences, Droevendaalsesteeg 3, 6708 PB Wageningen, the Netherlands

²Deltares, P.O. Box 177, 2600 MH Delft, the Netherlands

³Delft University of Technology, Faculty of Civil Engineering and Geosciences, P.O. Box 5, 2600 AA Delft, the Netherlands

⁴HKV, Botter 11-29, 8232 JN Lelystad, the Netherlands

Contents of this file

Text S1 to S4
Figures S1 to S7
Tables S1 to S2

Introduction

This document contains information on the numerical cases performed with the code ELV (S1), analysis on the impact of another choice of parameters (S2), a comparison between the damping length based on the temporal-mode analysis and spatial-mode analysis (S3) and two field cases to which the results are applied (S4).

Corresponding author: Hermjan Barneveld, (hermjan.barneveld@wur.nl)

Text S1 – Model cases

Table S1 shows the case names for the different simulations presented in Figures 8, 10, 11 and 13 of the manuscript.

Table S1. Cases performed in the study

	Cases, see legend in the Figures in the manuscript				
	$\Psi = 5.15 \text{ E-4}$				$\Psi = 2 \text{ E-4}$
	Perturbations theory, t=0yr	Perturbations long, t=0yr	Perturbations long, t=3yr	Perturbations large&long, Qwave, t=3yr	Perturbations theory, t=0yr
Froude number <i>F</i>	<i>Figures 8, 11, 13</i>	<i>Figures 8, 11, 13</i>	<i>Figures 8, 11, 13</i>	<i>Figures 8, 10</i>	<i>Figure 8</i>
0.13	006dXSS2bdyn	006dXSdyn	006dXSdyn	003d25Gdyn	006dXSS3bdyn
0.2	019dXSS2bdyn	019ddyn	019ddyn	013dxGdyn	019dXSS3bdyn
0.3	015dxSmXSS2bdyn	015dxSmdyn	015dxSmdyn	015dxGdyn	015dxSmXSS3dyn
0.4	017dXSS2cdyn	017ddyn	017ddyn	016dGdyn	017dXSS3dyn
0.5	016d5SmXSS2cdyn	016d5Smdyn	016d5Smdyn	016d5Gdyn	016d5SmXSS3dyn
0.6	011dx10aD35XSS2ddyn	018dadyn	018dadyn	011dx10aD35Gdyn	011dx10aD35XSS3dyn

For the assessment of the impact of the choice of the Chézy value on the migration celerity (while keeping the parameters F and Ψ equal), the following additional simulations have been performed ($F=0.2$ and $\Psi = 5.15\text{E-5}$).

- 013DXG2 with $C=40 \text{ m}^{1/2}/\text{s}$, $D50=0.009 \text{ m}$, $i_b=0.000245$ [-]
- 013DXG2a with $C=45 \text{ m}^{1/2}/\text{s}$, $D50=0.00633 \text{ m}$, $i_b=0.0001936$ [-].

Results of this analysis can be found in the Section S2 (Impact of the Chézy value).

The input and output of the model runs can be found in the Hydroshare Resource:

Barneveld, H. (2022). Supplementary information propagation of bed waves in rivers: ELV simulations and additional analyses, HydroShare,
<http://www.hydroshare.org/resource/7842147db84d4265b95fe2872132aa4a>

It contains the following documents:

- The Resource contains following files per case:
- beddev.xlsx - bed level as a function of time and space
- beddev_dyn_'name'.xlsx - analysis of beddev.xlsx to assess celerities and generate graphs
- cpu.txt - output cpu time simulation
- input.mat - Matlab input file for ELV
- log.txt - log file simulation
- output.mat - matlab output file ELV

Text S2 – Impact of the Chézy value

Changing the Chézy value, while maintaining the same values for water depth, velocity, Froude number F and transport parameter Ψ , requires changes in the bed slope and D_{50} , and causes changes in the parameter E . The linear stability analysis demonstrates the impact of these changes on the relative migration celerity and damping of bed waves. For small Froude numbers (<0.3) the impact of changes in bed slope, D_{50} and E on the migration celerity is negligible, as can be seen in Figure S1 (for $F \leq 0.3$ lines overlap).

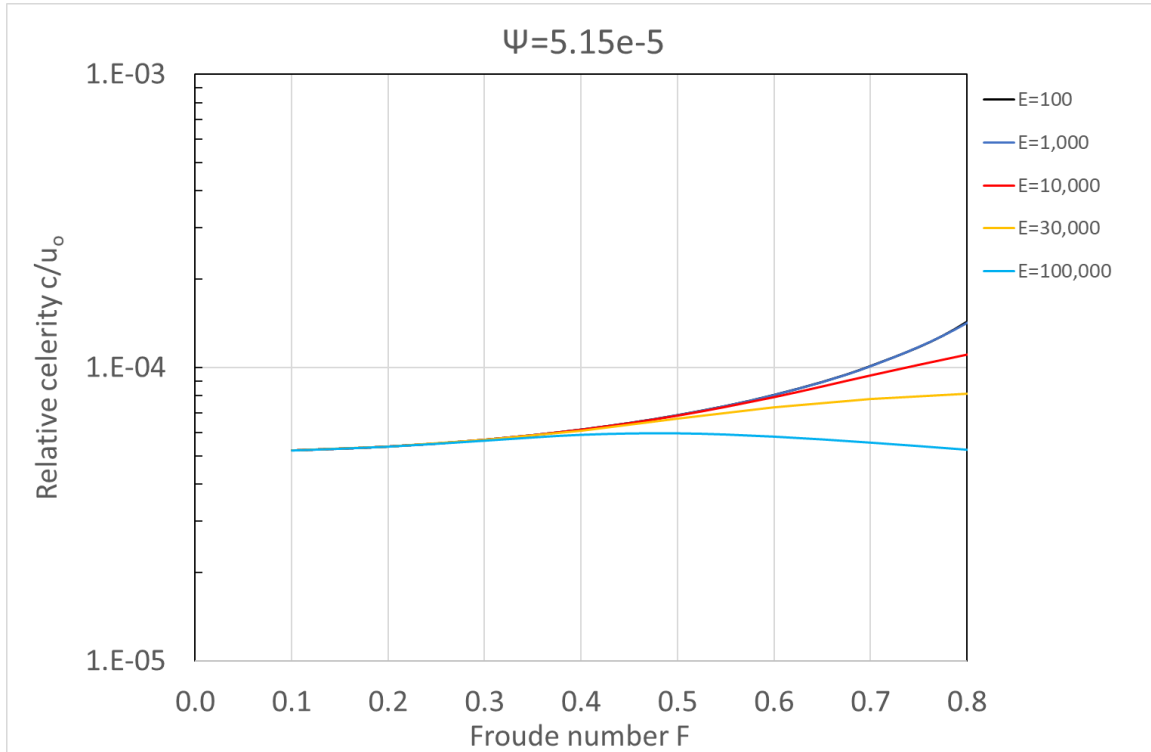


Figure S1. Relative celerity of bed waves in the linear stability analysis for $\Psi = 5.15 \cdot 10^{-5}$ (Figure 3 of manuscript).

We performed additional simulations in which we changed the Chézy value, as well as the values for i_b , and D_{50} so as to maintain the same values for F and Ψ . Table S2 gives the parameters as chosen, as well as the parameter values that result from these choices.

Table S2. Cases for sensitivity analysis for changed conditions for C , D_{50} and i_b .

parameter	Original simulation Case 013DXG2	Changed condition Case 013DXG2a
C (m ^{1/2} /s)	40	45
F (-)	0.2	0.2
Ψ (-)	5.15×10^{-5}	5.15×10^{-5}
i_b (slope)	0.000245	0.0001936
D_{50} (m)	0.009	0.00633

The results of both simulations, in terms of bed level change relative to the original bed slope ($i_{b,o}$), are presented in Figure S2. It can be seen that although the sediment loads appear to differ slightly, and the rates of diffusion in both simulations are somewhat different, the migration celerities (identified at the top of the wave) are almost identical. While keeping F and ψ the same, other choices of parameters yield identical results for the migration celerity of the wave, as long as the results are insensitive to changes in parameter E . This shows that the results of the linear stability analysis are valid, also in case of other parameter choices such as for the Chézy value.

The small differences in damping and diffusion may be due to numerical diffusion in ELV, which could be subject to further research.

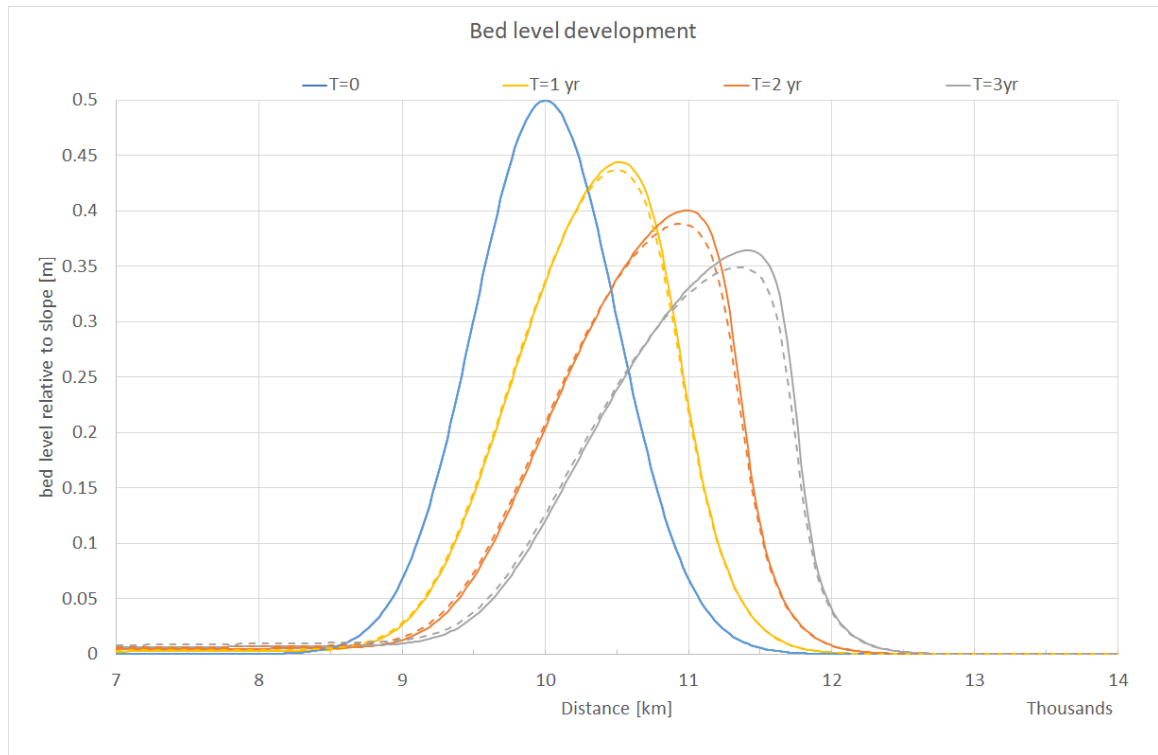


Figure S2. Comparison of dynamic of bed wave for alternative choices of C , D_{50} and i_b . Solid lines: base case 013DXG2; dashed lines: changed conditions case 013DXG2a.

Text S3 – Damping : Temporal-mode versus Spatial-mode

The damping or relaxation length are calculated in the spatial-mode analysis according to Eq. 16 in the main manuscript. For the temporal-mode analysis, the damping length can be calculated as follows. Suppose the peak of a wave travels with celerity c over a distance X . The corresponding travel time is $T_{Travel} = \frac{X}{c}$. The damping of the peak during this travel time is given by $\exp(\omega_i T_{Travel}) = \exp\left(\frac{\omega_i X}{c}\right)$, with damping factor ω_i and celerity c resulting from the temporal-mode analysis. This damping must also be equal to $\exp\left(-\frac{X}{L_D}\right)$, where L_D denotes the damping length. Hence, $\exp\left(\frac{\omega_i X}{c}\right) = \exp\left(-\frac{X}{L_D}\right)$, which implies $L_D = -\frac{c}{\omega_i}$.

Plotting this for the damping length L_D in Figure 11 of the manuscript provides Figure S3.

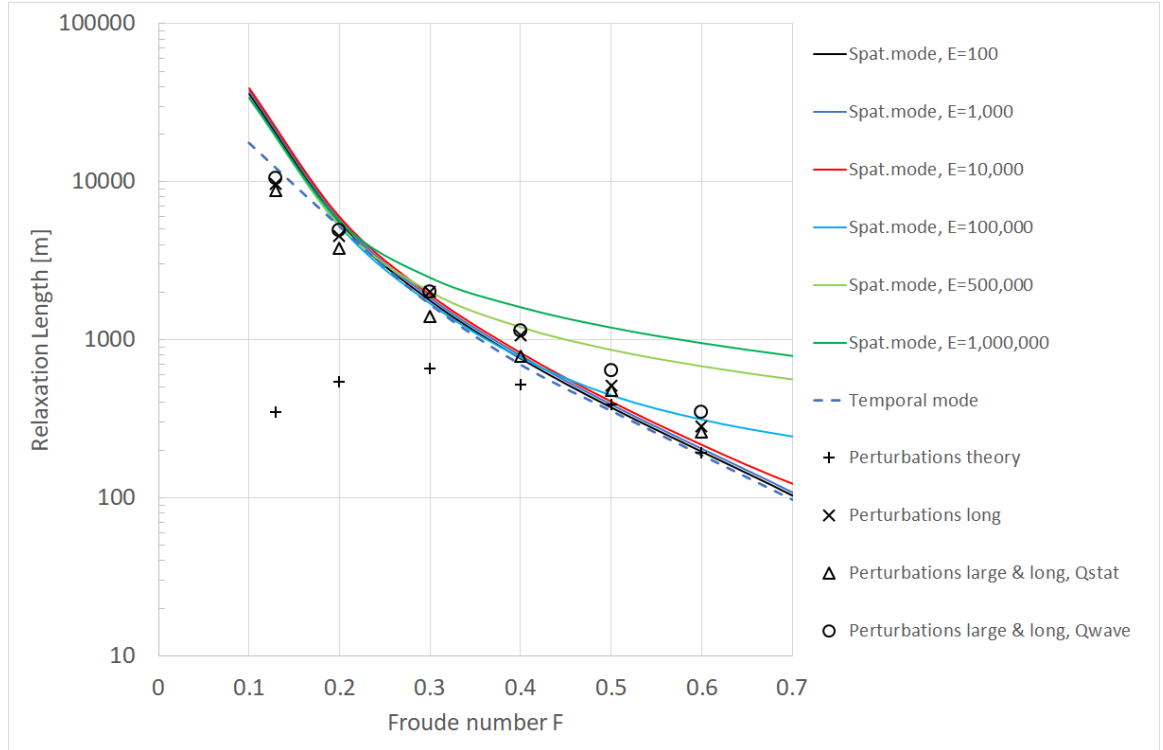


Figure S3. Comparison between damping of bed perturbations from linear stability analysis (solid lines for the spatial-mode, dotted line for the temporal-mode) and numerical simulations (markers) for $\psi = 5.15 \cdot 10^{-5}$. 'Perturbations theory' represent infinitesimal perturbations with a wave length coupled to the value of E . For the other simulations, the wave length increased to 3,000 m, while for 'Perturbations large & long, Qwave' the bed wave amplitude increased and a flood wave was applied.

The figure shows that the results from the temporal-mode analysis are close to those from the spatial-mode analysis, for values of the parameter E up to 1,000.

However, for low values of the Froude number ($F < 0.2$) the damping according to the temporal-mode analysis is somewhat larger (smaller value of L_D) than the damping from the spatial-mode analysis, and close to the numerical results for longer bed perturbations (x, Δ, o). For $F > 0.2$ the value of the parameter E in the spatial-mode analysis becomes important and the damping-length of the temporal-mode analysis appears to give the lower limit for both spatial-mode analysis results and the numerical results for long bed perturbations.

The comparison to numerical results needs further research, including the impact of numerical diffusion in ELV.

Text S4 – Field cases: Fraser River (Canada) and Waal River (the Netherlands)

To illustrate the applicability of the linear stability analysis results, two cases with relevant field data for rivers in Canada and the Netherlands are addressed.

Gold mining along the Fraser River between 1858 and 1909 added large amounts of sediment to the river's natural sediment load. Ferguson et al. (2015) and Nelson & Church (2012) reconstructed the impact of the additional sediment supplies on the morphodynamics.

The Waal River in the Netherlands is the main branch of the Rhine delta. The geometry of the river bed of the Waal River has been monitored every two weeks in the period 2005 and 2021. This monitoring material provides detailed information on the migration of bed waves with various wave lengths. Results of these analyses are documented by Gensen & van Denderen (2022).

Fraser River, Canada

The sediment pulse of place mining on the Fraser River has been analyzed by Ferguson et al. (2015) and Nelson & Church (2012) using observations of the Fraser River channel and numerical modelling. Based on these studies, the following data for the reach between Marguerite and Hope were extracted:

- An average bed slope i_0 of 0.001 (Ferguson et al., 2015);
- A steady dominant discharge of 7,000 m³/s operating 15% of the time predicts the total flux of sediment, grain size distribution and net morphological changes for a 20-year period with annual peaks ranging from 6,070 to 12,900 m³/s (Ferguson et al., 2015);
- An average channel width of 150 m (Ferguson et al., 2015);
- Froude numbers at mean annual flood of 0.45 at Hope and 0.56 at Marguerite (Nelson & Church, 2012);
- From 456 identified individual mines approximately 58,000,000 m³ of sediment was excavated, and dumped into the Fraser River between the Cottonwood Canyon (upstream of Marguerite) and Hope (Nelson & Church, 2012);
- An annual travel distance of placer mining sediment (L_b) varying between 1 and 6.3 km/yr, with a most likely value of 3.1 km/yr (Nelson & Church, 2012);
- An annual delivery value of 700,000 m³ of sediment, matching the most likely value of L_b (Nelson & Church, 2012).

These values were used in the linear stability analyses to assess the migration celerities, both for the spatial mode and the temporal mode approach. In those analyses, a Froude number of 0.5 was adopted as an average. As no information was readily available on flood wave periods (which determine parameter E in spatial mode analysis) and wave length L of the bed waves (parameter in temporal mode analysis) these parameters were varied (Figure S4). If the flood duration would be as long as 15% of time over a year (55 days), the parameter E would be approximately 19,000. Therefore, values of E larger than 100,000 are unlikely for the Fraser River. A bed wave with a wave

length L of 25 km or larger would slow down the bed wave to 1 km/yr, or less. Multiple bed waves (with shorter wavelengths, i.e. <10 km) may have moved through the system. Based on the latter assumptions, the migration celerities are in the range 2.25-3.3 km/yr (Figure S4).

The Froude numbers are larger than 0.3-0.4, and therefore, both transition and diffusion may be expected in this part for the Fraser River. Notwithstanding this expected behavior, we conclude that the results of both spatial mode and temporal mode analyses are close to the most likely bed wave migration celerity in this river (3.1 km/yr).

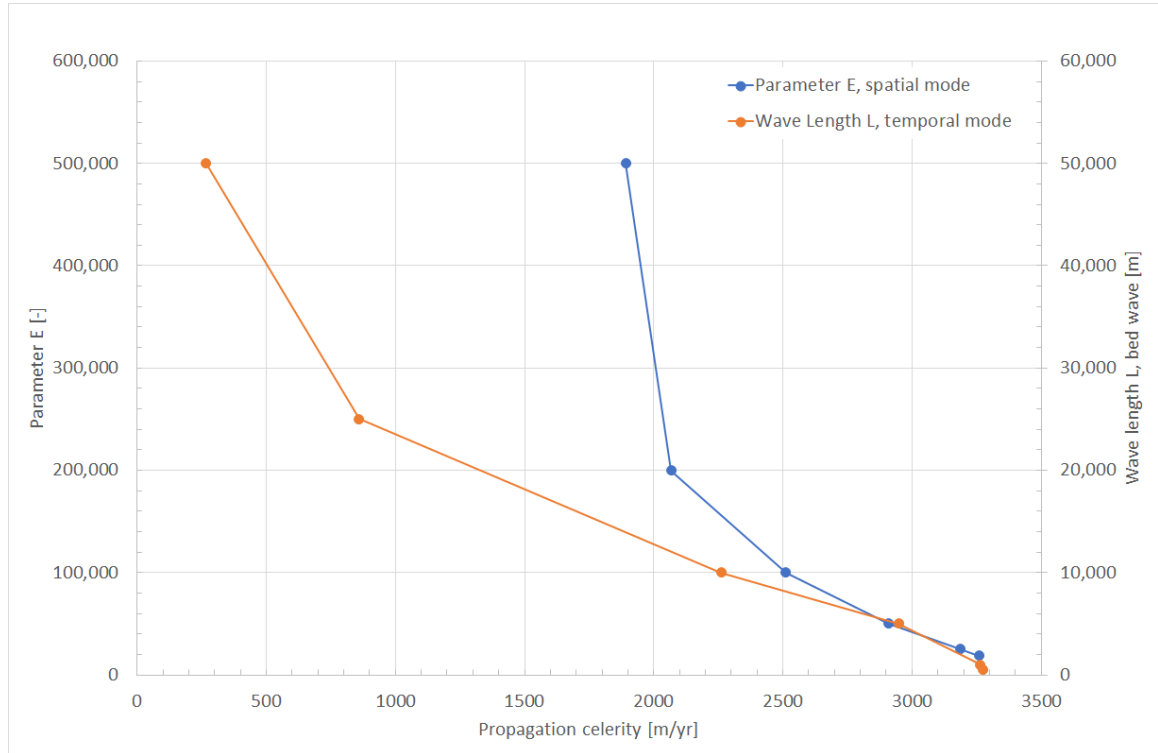


Figure S4. Sensitivity analysis on the impact of the parameter E (spatial mode analysis) and wave length bed wave L (temporal mode analysis) on the migration celerity of the bed wave. Fixed parameter settings are $i_0=0.001$, discharge $Q=7,000 \text{ m}^3/\text{s}$, channel width $W=150 \text{ m}$, annual sediment load $S=700,000 \text{ m}^3$ and Froude number $F=0.5$.

Waal River, The Netherlands

The Rhine River enters the Netherlands near the village of Lobith. After approximately 10 km, it bifurcates in the Waal River and the Pannerden Canal. The Waal River flows to the west towards the Rhine-Meuse Delta, in which the large harbor of Rotterdam is situated. The Waal River and Rhine River are of high importance for navigation. The riverbed of these rivers is monitored frequently to assess the navigation depth and to plan dredging activities. In the period 2005-2021, the bed level of the navigation channel has been monitored every two weeks, which means that a large database is available to analyze morphodynamics of the river.

Van Denderen et al. (2022) use these detailed bed level measurements to study the morphological changes on multiple scales using a wavelet transform. A wavelet transform distinguishes and disentangles the bed-level changes on different spatial scales. In this way, the bed level change caused by a local intervention can be separated from larger scale changes. Gensen and Van Denderen (2022) applied this method to filter out bed waves with lengths between 300 m and 4 km. Such bed waves may be initiated by changes in river geometry, combined with flood events. These bed waves subsequently migrate downstream. An example of the result of the wavelet tool can be seen in Figure S5, clearly showing the downstream migration of longer bed waves.

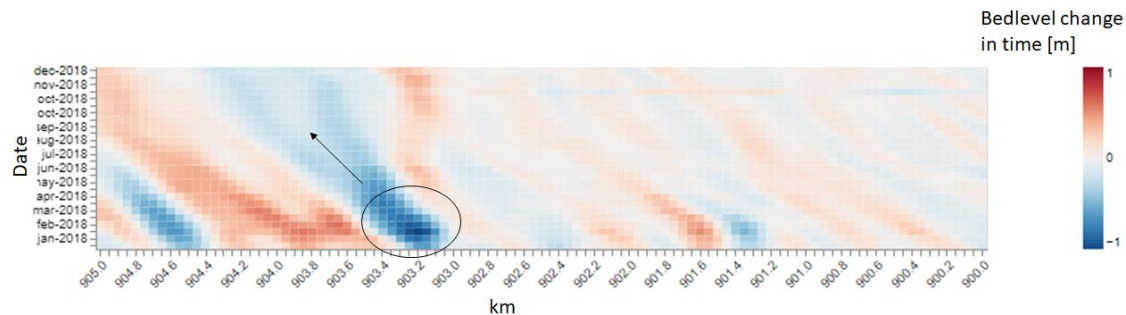


Figure S5. Bed level change for part of the Waal River in the year 2018. Clearly, the downstream migration of bed level peaks (red) and troughs (blue) can be distinguished. Water flows from right to left. Source: Van Denderen and Van Hoek (2022).

For comparison of the observed migration celerities, with results of the linear stability analyses, we selected a part of the Waal River which is called the Middle Waal in the reach km 887-915, see Figure S6. This reach is relatively straight and the migration celerities appear to be quite stable in time. For this section, Gensen & Van Denderen (2022) determined an annual travel distance of the bed waves varying between 1.1 and 1.4 km/yr .



Figure S6. Rhine and Waal River in the Netherlands. The Rhine enters the Netherlands near Lobith. Downstream from the bifurcation at the Pannerdensche Kop (km 867.5) the Waal River flows to the West. Downstream from the city of Nijmegen, the river is called the Middle-Waal.

Frings et al. (2019) provide an estimate of the annual sediment load for the Waal River of 200,000 m³ excluding pores ($\pm 50\%$), or 333,333 m³ ($\pm 50\%$) including pores. Other input parameters for the linear stability analyses are based on the discharge time-series at

Lobith (Figure S7) for the period 2005-2021. This time-series is transformed into representative discharges, specific discharges (m^2/s), water depths, flow velocities and Froude numbers based on:

1. The distribution of the river discharge at the bifurcation;
2. Water level slope;
3. Average cross-sectional shape containing width of the main section, relative height of the groynes and floodplains;
4. The discharge distribution in the cross-sectional profile (main section, groyne section, floodplain) extracted from numerical model results.

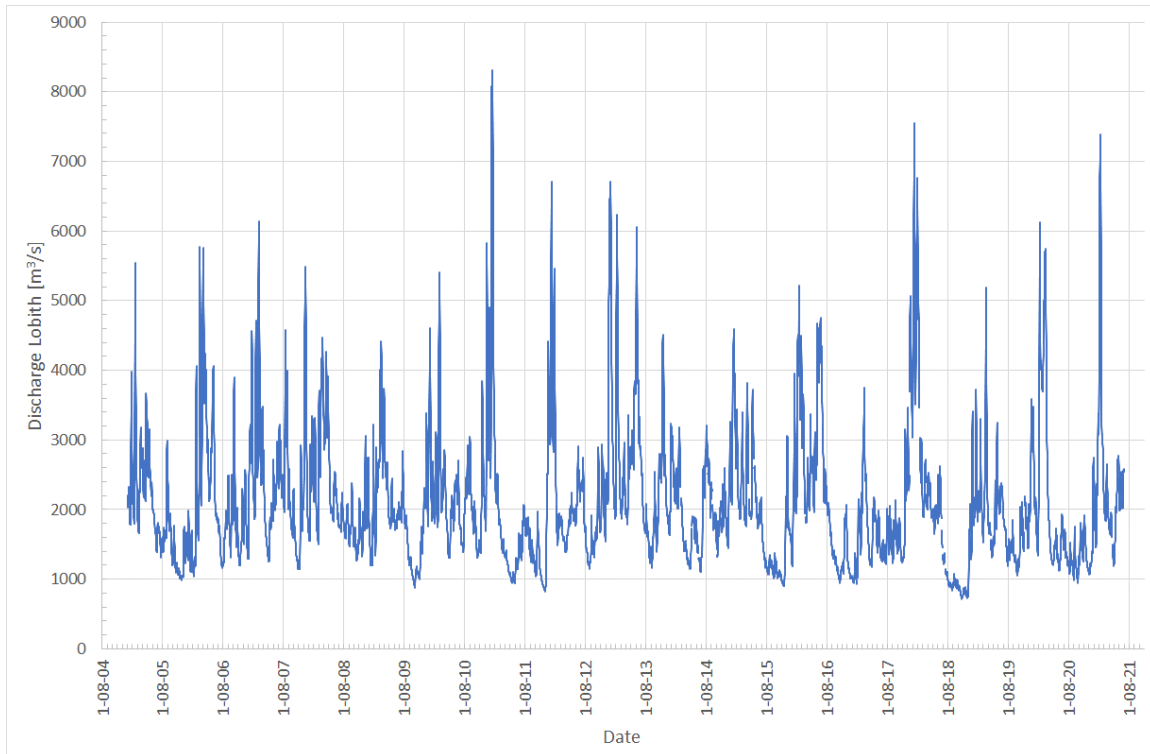


Figure S7. Discharge time-series at Lobith for the period January 2005 to July 2021.

This information, combined with river characteristics from Paarlberg & Schippers (2020), yields the following input parameters for the linear stability analyses:

- An average bed slope i_o of 1.10^{-4} ;
- The average discharge at Lobith in the observation period is approximately $2,000 \text{ m}^3/\text{s}$. For the analyses we adopted this discharge level as well as discharge levels of $1,600 \text{ m}^3/\text{s}$ (overtopping of groynes) and $3,000 \text{ m}^3/\text{s}$;
- With information from Paarlberg & Schippers (2020), for the three discharge levels ($1,600$, $2,000$ and $3,000 \text{ m}^3/\text{s}$), we determined the corresponding total discharges in the Waal ($1,268$, $1,461$ and $2,049 \text{ m}^3/\text{s}$), the discharges in the

main river (between the groynes) (1,268, 1,432 respectively 1,900 m³/s), and water depth (5, 5,5 and 6,5 m);

- An average channel width of 253 m;
- Froude number of 0.15;
- An annual sediment load of 333,333 m³.

Based on this input, the wave celerities in both spatial mode and temporal mode analysis were calculated. We varied the characteristic discharge at Lobith (and the Waal River) and the wave length of the bed wave. Figure 2 in the manuscript shows that for Froude numbers of 0.15, the results are insensitive to the value of the parameter E .

The results with varying wave length L of the bed wave (a parameter only in temporal mode) showed insensitivity in the range $L=300-4000$ m. The discharge at Lobith does exert an influence. When the annual sediment load remains unchanged (333,333 m³/yr), the travel distance L_b is 1,345 m/yr when the discharge at Lobith is 1,600 m³/s. For discharges at Lobith equal to 2,000 m³/s (mean discharge) and 3,000 m³/s, L_b reduces to 1,222 and 1,035 m/yr, respectively. Differences in results of the spatial mode and temporal mode are negligible.

Choosing an average discharge (2,000 m³/s) apparently provides a good approximation of the observed annual travel distance of 1.1 and 1.4 km/yr. Adopting low (1,600 m³/s) or high (3,000 m³/s) estimates of the discharge at Lobith yield bed wave celerities matching the observed values, but at the borders of the band width of the observations. It should be realized that the annual sediment load was identical for the three discharge values (333,333 m³/yr). It can be concluded that adopting a correct value for the annual sediment load is more important than the selected value of the discharge, as the celerity appears to be linearly dependent on the sediment load.

REFERENCES

Ferguson, R. I., M. Church, C. D. Rennie, and J. G. Venditti (2015), Reconstructing a sediment pulse: Modeling the effect of placer mining on Fraser River, Canada, J. Geophys. Res. Earth Surf., 120, 1436–1454, doi:10.1002/2015JF003491.

Frings, R. M., G. Hillebrand, N. Gehres, K. Banhold, S. Schriever, and T. Hoffmann (2019), From source to mouth: Basin-scale morphodynamics of the Rhine River, Earth-science reviews 196: 102830.

Gensen M. and R.P. van Denderen (2012), Propagation celerity bed disturbances using bed level soundings Rhine and Waal, in Dutch: "Loopsnelheid bodemverstoringen - Op basis van vaargeulpeilingen Bovenrijn/Waal", Report HKV, PR4597.10, March 2022.

Nelson A.D. and M. Church (2012), Placer mining along the Fraser River, British Columbia: The geomorphic impact, Geological Society of America Bulletin; July/August 2012; v. 124; no. 7/8; p. 1212–1228; doi: 10.1130/B30575.1

Paarlberg A. and M. Schippers (2020), Inverse modelling equilibrium effect of measures on main river bed: deriving dimensions of measures, In Dutch: "Inverse modellering evenwichtseffect maatregelen op zomerbedbodem: afleiden dimensies van maatregelen", 22 January 2020.

Van Denderen R. P. and M. van Hoek (2022), Wavelet application, Help documentation, in Dutch: "Waveletapplicatie, Helpdocumentatie", Report HKV, PR4591.10, March 2022.

Van Denderen R. P., E. Kater, L. H. Jans, and R.M. Schielen (2022), Disentangling changes in the river bed profile: The morphological impact of river interventions in a managed river. Geomorphology, 408, 108244.